A UNITED STATES DEPARTMENT OF COMMERCE PUBLICATION

# NOAA Technical Memorandum NWS WR77

U.S. DEPARTMENT OF COMMERCE
National Oceanic and Atmospheric Administration
National Weather Service

# A Study of Radar Echo Distribution in Arizona During July and August

JOHN E. HALES, JR.

estern Region

ALT LAKE CITY,
UTAH

July 1972

NOAA TECHNICAL MEMORANDA

National Weather Service, Western Region Subseries

The National Weather Service (NWS) Western Region (WR) Subseries provides an informal medium for the documentation and quick dissemination of results not appropriate, or not yet ready, for formal publication. The series is used to report on work in progress, to describe technical procedures and practices, or to relate progress to a limited audience. These Technical Memoranda will report on investigations devoted primarily to regional and local problems of interest mainly to personnel, and hence will not be widely distributed.

Papers 1 to 23 are in the former series, ESSA Technical Memoranda, Western Region Technical Memoranda (WRTM); papers 24 to 59 are in the former series, ESSA Technical Memoranda, Weather Bureau Technical Memoranda (WBTM). Beginning with 60, the papers are part of the series, NOAA Technical Memoranda NWS.

Papers 1 to 23, except for 5 (revised edition) and 10, are available from the National Weather Service Western Region, Scientific Services Division, P. O. Box 11188, Federal Building, 125 South State Street, Salt Lake City, Utah 84111. Papers 5 (revised edition), 10, and all others beginning with 24 are available from the National Technical Information Service, U.S. Department of Commerce, Sills Bldg., 5285 Port Royal Road, Springfield, Va. 22151. Price: $3.00 paper copy; $0.95 microfiche. Order by accession number shown in parentheses at end of each entry.

ESSA Technical Memoranda

WRTM 1 Some Notes on Probability Forecasting. Edward D. Diemer, September 1965. (Out of print.)

WRTM 2 Climatological Precipitation Probabilities. Compiled by Lucianne Miller, December 1965.

WRTM 3 Western Region Pre- and Post-FP-3 Program, December 1, 1965 to February 20, 1966. Edward D. Diemer, March 1966.

WRTM 4 Use of Meteorological Satellite Data. March 1966.

WRTM 5 Station Descriptions of Local Effects on Synoptic Weather Patterns. Philip Williams, Jr., April 1966 (revised November 1967, October 1969). (PB-178000)

WRTM 6 Improvement of Forecast Wording and Format. C. L. Glenn, May 1966.

WRTM 7 Final Report on Precipitation Probability Test Programs. Edward D. Diemer, May 1966.

WRTM 8 Interpreting the RAREP. Herbert P. Benner, May 1966 (revised January 1967). (Out of print.)

WRTM 9 A Collection of Papers Related to the 1966 NMC Primitive-Equation Model. June 1966.

WRTM 10 Sonic Boom. Loren Crow (6th Weather Wing, USAF, Pamphlet), June 1966. (Out of print.) (AD-479366)

WRTM 11 Some Electrical Processes in the Atmosphere. J. Latham, June 1966.

WRTM 12 A Comparison of Fog Incidence at Missoula, Montana, with Surrounding Locations. Richard A. Dightman, August 1966. (Out of print.)

WRTM 13 A Collection of Technical Attachments on the 1966 NMC Primitive-Equation Model. Leonard W. Snellman, August 1966. (Out of print.)

WRTM 14 Application of Net Radiometer Measurements to Short-Range Fog and Stratus Forecasting at Los Angeles. Frederick Thomas, September 1966.

WRTM 15 The Use of the Mean as an Estimate of "Normal" Precipitation in an Arid Region. Paul C. Kangieser, November 1966.

WRTM 16 Some Notes on Acclimatization in Man. Edited by Leonard W. Snellman, November 1966.

WRTM 17 A Digitalized Summary of Radar Echoes Within 100 Miles of Sacramento, California. J. A. Youngberg and L. B. Overaas, December 1966.

WRTM 18 Limitations of Selected Meteorological Data. December 1966.

WRTM 19 A Grid Method for Estimating Precipitation Amounts by Using the WSR-57 Radar. R. Granger, December 1966. (Out of print.)

WRTM 20 Transmitting Radar Echo Locations to Local Fire Control Agencies for Lightning Fire Detection. Robert R. Peterson, March 1967. (Out of print.)

WRTM 21 An Objective Aid for Forecasting the End of East Winds in the Columbia Gorge, July through October. D. John Coparanis, April 1967.

WRTM 22 Derivation of Radar Horizons in Mountainous Terrain. Roger G. Pappas, April 1967.

WRTM 23 "K" Chart Applications to Thunderstorm Forecasts Over the Western United States. Richard E. Hambidge, May 1967.

ESSA Technical Memoranda, Weather Bureau Technical Memoranda (WBTM)

WBTM 24 Historical and Climatological Study of Grinnell Glacier, Montana. Richard A. Dightman, July 1967. (PB-178071)

WBTM 25 Verification of Operational Probability of Precipitation Forecasts, April 1966-March 1967. W. W. Dickey, October 1967. (PB-176240)

WBTM 26 A Study of Winds in the Lake Mead Recreation Area. R. P. Augulis, January 1968. (PB-177830)

WBTM 27 Objective Minimum Temperature Forecasting for Helena, Montana. D. E. Olsen, February 1968. (PB-177827)

WBTM 28 Weather Extremes. R. J. Schmidli, April 1968 (revised July 1968). (PB-178928)

WBTM 29 Small-Scale Analysis and Prediction. Philip Williams, Jr., May 1968. (PB-178425)

WBTM 30 Numerical Weather Prediction and Synoptic Meteorology. Capt. Thomas D. Murphy, U.S.A.F., May 1968. (AD-673365)

WBTM 31 Precipitation Detection Probabilities by Salt Lake ARTC Radars. Robert K. Belesky, July 1968. (PB-179084)

WBTM 32 Probability Forecasting--A Problem Analysis with Reference to the Portland Fire Weather District. Harold S. Ayer, July 1968. (PB-179289)

WBTM 33 Objective Forecasting. Philip Williams, Jr., August 1968. (AD-680425)

WBTM 34 The WSR-57 Radar Program at Missoula, Montana. R. Granger, October 1968. (PB-180292)

WBTM 35 Joint ESSA/FAA ARTC Radar Weather Surveillance Program. Herbert P. Benner and DeVon B. Smith, December 1968 (revised June 1970). (AD-681857)

WBTM 36 Temperature Trends in Sacramento--Another Heat Island. Anthony D. Lentini, February 1969. (Out of print.) (PB-183055)

WBTM 37 Disposal of Logging Residues Without Damage to Air Quality. Owen P. Cramer, March 1969. (PB-183057)

WBTM 38 Climate of Phoenix, Arizona. R. J. Schmidli, P. C. Kangieser, and R. S. Ingram. April 1969. (Out of print.) (PB-184295)

WBTM 39 Upper-Air Lows Over Northwestern United States. A. L. Jacobson, April 1969. (PB-184296)

WBTM 40 The Man-Machine Mix in Applied Weather Forecasting in the 1970s. L. W. Snellman, August 1969. (PB-185068)

WBTM 41 High Resolution Radiosonde Observations. W. S. Johnson, August 1969. (PB-185673)

WBTM 42 Analysis of the Southern California Santa Ana of January 15-17, 1966. Barry B. Aronovitch, August 1969. (PB-185670)

WBTM 43 Forecasting Maximum Temperatures at Helena, Montana. David E. Olsen, October 1969. (PB-185762)

WBTM 44 Estimated Return Periods for Short-Duration Precipitation in Arizona. Paul C. Kangieser, October 1969. (PB-187763)

WBTM 45/1 Precipitation Probabilities in the Western Region Associated with Winter 500-mb Map Types. Richard A. Augulis, December 1969. (PB-188248)

U. S. DEPARTMENT OF COMMERCE
NATIONAL OCEANIC AND ATMOSPHERIC ADMINISTRATION
NATIONAL WEATHER SERVICE

NOAA Technical Memorandum NWSTM WR-77

# A STUDY OF RADAR ECHO DISTRIBUTION IN ARIZONA DURING JULY AND AUGUST

John E. Hales, Jr.
Weather Service Forecast Office
Phoenix, Arizona

WESTERN REGION
TECHNICAL MEMORANDUM NO. 77

SALT LAKE CITY, UTAH
JULY 1972

TABLE OF CONTENTS

## LEGENDS FOR FIGURES

LEGENDS FOR FIGURES (Continued)

LEGENDS FOR FIGURES (Continued)

# A STUDY OF RADAR ECHO DISTRIBUTION IN ARIZONA DURING JULY AND AUGUST


## ABSTRACT

Arizona's summer thunderstorm regime differs from that of any other section of the country. The mountainous sections of the state, notably the White Mountains northwestward to the San Francisco Peaks, have one of the highest frequencies of afternoon thunderstorms in the United States. The desert valleys of Arizona, particularly around Phoenix, have a diurnal regime of thunderstorm activity which is diametrically opposite to that of the mountainous country located less than 100 miles to the north and northeast. Forty-eight percent of the thunderstorms that occur in Phoenix are observed in the period from 1800 to 2400 MST. This is one of the highest percentage frequency of occurrences at this time of day in the United States.

Hourly composite radar charts for the summer months of July and August of 1970 and 1971 were prepared for the greater part of Arizona. These charts clearly illustrate the very pronounced diurnal regime that the thunderstorm activity follows. During the late morning through early afternoon, thunderstorms are confined to the highest mountains. By late afternoon maximum activity shifts into foothills adjacent to deserts and remains in this area until late evening when there is little organization to the distribution.

An analysis was also made of the change of thunderstorm distribution between hours. This more clearly illustrates the progression of thunderstorms from the higher mountains in the early afternoon into the deserts by evening.


## I. INTRODUCTION

Radar provides one of the best means for studying areal and temporal distribution of summertime showers and thunderstorms (radar echoes).

Good coverage of radar data has only been available for Arizona since 1970. Therefore, this type of study should provide a greater understanding of the very important thunderstorm season in Arizona.

Due to the scarcity of observing stations, widely differing terrain elevations, and a true airmass-type thunderstorm pattern, the summer convective shower regime in Arizona can be adequately studied only by use of radar surveillance.

For this study, only the months of July and August were investigated. June normally is a dry month while September is a month of transition with the middle latitude westerlies occasionally affecting the state.

The months of July and August are dominated almost entirely by airmass-type convective activity with only temporary periods of drying.

Terrain elevation plays a very important role as this study will reveal. As a general rule the locale of maximum convective activity varies with the time of day. The highest mountains reach their peak of activity early in the afternoon while the desert valleys, particularly around Phoenix, do not peak until near midnight.

This study will clearly show this transition as well as raise many questions concerning the thermodynamic mechanisms involved.

## II. DATA

Radar data for July and August 1971 were taken from the radar facsimile charts transmitted by National Weather Service (NWS) units located at Air Route Traffic Control (ARTC) centers in Albuquerque, Salt Lake City, and Palmdale. A 15x13 gridded overlay of 23 nm squares was placed over each hourly radar chart and a notation was made of squares that contained at least one echo. Under this procedure, no account was made of the amount of coverage of each square; also intensity was not considered since ARTC radar does not readily detect differences in echo strength. For the July-August period, a tabulation was made of the number of times echoes were observed in each square for each hour of the day. This data was then converted to a percentage representing the frequency of echo occurrence, by hour, in each grid square over the July-August period. The total grid covers all of Arizona except strips along the western and northern borders. This technique is the same as that used in a study of thunderstorms in Florida (Smith 1970).

The radar sites used, Figure (1), cover most of the grid. Coverage varies with height and intensity of precipitation cells and also with the type of polarization being used; linear or circular. Circular polarization tends to eliminate all but the heaviest precipitation cells. The FAA uses circular polarization only when there is so much precipitation showing on the scope that aircraft tracking is hindered. No attempt was made to differentiate between the type of polarization in use in the anlyses since most of the cells in the summer are strong enough to be displayed even in the circular mode (Benner and Smith, 1968); also the concern was only if any part of a square contained an echo. Data from Mt. Laguna radar site was not available from 2200 MST to 0600 MST. However this only affected the detection in the southwest corner of the grid, the area of least interest due to the low frequency of activity. There were a few occurrences of spurious echoes that were not weather related. Most of these were identified as such and not used.

## III. ANALYSES

From the raw data four different types of analyses were made:

1. Hourly frequency of echo detection
2. Three-hourly change in echo frequency
3. Graph of echo frequency for selected locations
4. Twenty-four hour mean echo frequency.

All of the above analyses will be used in a description of the daily fluctuation of echo coverage in the grid area. A grid square was only checked to see if one or more echoes were located in it, in order to ascertain if airmass characteristics were favorable at that time in that location to support convective activity. For this reason the amount of coverage was not considered. The grid used encompasses most of Arizona, a small section of Sonora, Mexico, and a very small portion of northwestern New Mexico.

Figures 2 through 25 portray hourly convective activity during the 24-hour period 0930 MST to 0830 MST inclusive.

Figure 2, for 0930 MST, which was the hour of least echo detection, shows the only activity of significance located over the Coconino Plateau with frequency maximum of 10%. The next chart, 1030 MST, displays an increase in frequency over the White Mountains and the San Francisco Mountains. At 1130 MST, the maximum in each of these areas shows a strong preference for the east slopes of the mountains rather than over the highest peaks. Also at this time, a sharp increase in frequency is noted over the Coconino Plateau and Juniper Mountains to the northwest of Prescott.

At 1230 MST, the axis of maximum frequency continues to be closely related to the east slopes of the mountains, with a general increase noted in all the mountain country of northern and eastern Arizona. One point of interest is the frequency decrease of 10% observed at both San Francisco Peaks and Escudilla Mountains (along the Arizona-New Mexico border) since 1130 MST. This decrease may be due to early cloud cover which limited convection temporarily. However, activity did redevelop after noon and reached its peak at both sites about 1430 MST before subsiding. The point graph for Escudilla Mountain, Figure 26, shows this trend in activity quite well.

The highest point frequency of the entire analysis, 67% was reached at 1330 MST in an area just southeast of Flagstaff. One of the surprising features of this study is that, except for the hour of 1130 MST, the maximum frequency on the grid from 1030 MST to 1730 MST is located in the quadrant to the south of Flagstaff, rather than over tha adjacent higher terrain. This feature is further substantiated by the 24-hour mean frequency chart, Figure 27, which shows that the area immediately south of Flagstaff has a higher frequency than any other area on the map.

Two reasons are advanced for this apparent anomaly. First, the prevailing, high level, or steering winds are south or southeast during July and August, and therefore nearly parallel to the Mogollon Rim. These winds tend to keep thunderstorm activity from drifting toward lower elevations and keep it concentrated along the higher terrain. Second, and perhaps more important, the Mogollon Rim, in the Flagstaff area, has a substantial slope to both west and northeast. This topography favors convergence of upslope winds from both of the steep slopes during the afternoon. Within this regime, the San Francisco Mountains are nearly a point source of convective activity with upslope flow in the afternoon on all slopes.

Figure 7 for 1430 MST indicates a shift in the axis of maximum frequency toward the southwest edge of the Mogollon Rim and White Mountains. The three-hour frequency change chart for 1430 MST, Figure 29, clearly illustrates this shift. The two most significant frequency changes are noted over McNary and just west of Heber. The frequency change maximum, which develops over the Escudilla Mountains at 1030 MST appears to move west-southwest about 150 miles to a point over the desert floor near Casa Grande about eight hours later (Figure 33). The unusual feature of this movement is that it is almost perpendicular to the direction of the mean steering level winds which are from the southeast. Further, from the echo frequency change charts, Figures 28 through 35, it appears that a bodily movement of the convective activity took place to a valley area and was not a discontinuous shift from one mountainous complex to another.

Also at 1430 MST (Figure 7), the echo frequency chart shows a pronounced minimum of activity over the desert floor in the Salt River Valley. This null point in activity occurs near the time of maximum surface heating in this area. This poses a question about the mechanism for desert thunderstorms, since very high surface temperatures apparently are not a vital factor in the release of convective energy over the desert floor.

The remainder of the echo frequency charts from 1530 MST to 1830 MST show persistence of activity in the mountainous areas and very low frequencies over the deserts. However a few items are worthy of amplification. In this period there appears to be a continued, although rather subtle, shift of the frequency maximum to the southwest from the Mogollon Rim. The maximum frequency south of Flagstaff remains in place until about 1730 MST (Figure 10). The 10% frequency isopleth closely follows the boundary between desert and mountainous terrain, although by 1830 MST it has moved further into the desert area.

While some increase in activity is noted in the mountainous areas of southeastern Arizona, an area of less than 10% frequency is apparent at 1530 MST in the valleys near the southeastern border. The frequency in this area increases briefly at 1630 MST and 1730 MST and then subsides again. The terrain in this area is mainly below 4000 feet above sea level and is a rather flat valley approximately 60 miles wide. The point graph for Clifton (Figure 36) located in this valley portrays a sharp increase in radar echoes near the time of

maximum heating and a rapid decrease by sunset. This variation is not prominent in other low-lying areas of the state and suggests a close coupling with thundershower activity in the adjacent mountains.

The charts for 1730 MST and 1830 MST show a noticeable trend for decreasing activity over the higher mountain country, with a shift towards increasing frequency change to the adjacent valley areas. This trend suggests that mountain thunderstorm activity, at least, follows the classical pattern of convection closely associated with insolation.

At 1930 MST, decreasing frequencies are apparent in all but a few sections of the map. The desert area from north of Phoenix to near Tucson is one area of increase. Two other areas of increasing frequency are noted in the San Pedro Valley of southeastern Arizona, and near Winslow in the northeastern part of the state. By 2030 MST, the highest frequencies are concentrated in an area from the southeast portion of the grid, northward to the Mogollon Rim, and then westward to near Prescott. The higher mountains continue to show a decrease. The peak of activity at this time is concentrated in the southeast, near Douglas. This pattern fits the point graph for Douglas, Figure 37, which shows one maximum about 1630 MST and a second about 2030 MST.

The frequency change chart for 2030 MST, Figure 35, shows a small increase of activity from Tucson northwestward to the desert valleys near Phoenix. The center of maximum increase has moved from near Florence to about the Chandler area by 2030 MST.

From 2130 MST to 2330 MST, Figures 14 through 16, the pattern of frequencies over the grid becomes rather disorganized, lacking the pronounced gradients noted on the afternoon charts. Higher values persist over some of the mountain areas but they are markedly lower than the afternoon values. However, the fact that activity does tend to persist in sections of the Mogollon Rim suggests an additional element other than surface heating as a factor in thunderstorm activity.

During the hours 0030 MST to 0230 MST, the frequency maximum shifts from the Mogollon Rim southwestward to a position over the desert valley between Phoenix and Florence. The frequency over this south-central desert area increases to 15%, while values on the remainder of the grid decrease to 10% or less. The area around Phoenix reaches its peak of activity at 0130 MST to 0230 MST, and the point graph for Phoenix, Figure 38, shows this quite clearly.

An interesting feature shows up when the frequency chart for 1430 MST, Figure 7, is compared with the one for 0230 MST, Figure 19. The distribution of frequencies reverses itself in this 12-hour period, and clearly shows an afternoon peak over mountain areas and the nighttime peak over the deserts. This serves to emphasize the point that convective activity, in Arizona at least, results from more complex mechanisms than the classical concept of cumulonimbus being generated by surface heating alone in a moist, unstable airmass.

The period 0530 MST to 1030 MST is shown in Figures 22 through 25, and Figures 2 and 3. Only the western portion of the grid displays frequencies of more than 5%. During this period there appears to be a shift in the 5% maximum from near Phoenix and Gila Bend to the north and northwest toward Kingman, eventually developing a center of 10% frequency over the Coconino Plateau at 0930 MST.

It is also noteworthy that an increase in activity, albeit rather small, is observed in the extreme southwest corner of the grid in Sonora, Mexico. Prior to 0530 MST, this area was marked by near zero frequencies during the afternoon and nighttime hours. Apparently, the effect of the afternoon sea breeze from the Gulf of California, just to the south of this area, and the notable lack of any high terrain in this part of Sonora, both tend to limit the convective activity that might result from surface heating alone. However, the late night and early morning hours seem to favor radiation from the top of the high-level moist layer and this may be the prime mechanism in the release of convection.

One of the questions that comes to mind is: How valid is one year's data in comparison to the diurnal distribution of echo frequency that could be expected over a period of several years?

A partial study was done for July and August 1970 for several hours using only data from the Phoenix and Silver City radar scopes. For comparison between 1970 and 1971 data, only the portion of the grid with good coverage from the Phoenix and Silver City scopes was used.

Comparing the 1430 MST frequency for 1970, Figure 39, with the same time in 1971, Figure 7, it is evident that there are only minor differences. The axis of maximum frequency is located on the Mogollon Rim and White Mountains on both charts with a secondary axis extending northward just to the east of Tucson. The desert valleys around Phoenix both years are near zero frequency. Also an area of 5% or less is evident on both charts south of the White Mountains.

At 1730 MST both charts are very similar, Figures 10 and 40. The one very surprising similarity is the distinct area of maximum frequency located at exactly the same point on both charts, just west of San Carlos. If this area was located over a high mountain or some orographically favored location, it wouldn't be so unusual. However, this area of maximum frequency is located over a relatively flat basin. As was noted in the 1971 survey, this maximum also appears to have moved west-southwestward off the White Mountains. There is a frequency minimum for 1970 over the White Mountains with a small maximum noted in the same area in 1971. Overall the frequencies are higher over the grid during 1971, indicating a more active year.

At 2030 MST, Figures 13 and 41, the centers of maximum echo frequency are similar in both years. There is a maximum in the vicinity of

Prescott on both charts with another maximum frequency area to the east of Tucson. The area of greatest frequency is near San Carlos (Figure 41), having moved west-southwest since 1730 MST (Figure 40). A minimum frequency center is located south of the White Mountains in both years, though more pronounced in 1971. There is very little difference between the two years over the desert valley near Phoenix.

Comparing the 2330 MST charts, Figures 16 and 42, the only strong similarities are the lack of echo detection in the White Mountains and the higher frequencies extending from west of Show Low southwestward toward the Globe area. The maximum frequency centers, however, differ with 1970 having the centers near Superior while in 1971 the primary center was located northwest of San Carlos. The desert valleys from Phoenix east and southeast differ little except for less activity in 1971 from Florence southward to the northwest of Tucson.

At 0230 MST, Figures 19 and 43, the concentration of activity differs quite a bit. In 1970 two areas of maximum frequency are apparent. The first is from near Wickenburg northeast to the Verde Valley with the other small area over the mountains east of Tucson. In 1971 the maximum frequency center was located in the desert near Florence with a small center near Prescott. Both years again indicated little activity in the White Mountains and the valleys immediately to the south.

## IV. CONCLUSIONS

There are many uses that this type of study can be put to, particularly in data-sparce areas such as Arizona.

Radar climatology of mean frequency charts by hour and day can be used to supplement present climatological data on thunderstorms now available, particularly in data-sparce areas.

By comparing selected point graphs from the radar data with the hourly variation of measurable precipitation for July and August at corresponding locations (Sellers and Green 1964), the similarities are readily apparent, Figure 44 (Sellers data for period 1948-57). Note that the time of maximum frequencies for both curves are very similar.

For aviation forecasting, prediction of the onset of thunderstorm activity during the day as well as termination time can be kept within certain limits, depending on climatological echo frequency distribution. For example, when forecasting for Winslow it would be unwise to expect thunderstorm activity to continue beyond 2100 MST whereas at Phoenix, thunderstorms should seldom be forecast before 1700 MST. On the other hand an increasing likelihood of thunderstorms can be expected at Phoenix between 1700 MST and midnight.

Another obvious usage would be in fire-weather forecasting where the beginning and ending of thunderstorms are a critical factor in many situations.

In hydrology this type of data is already being used to supplement rainfall reports for the purpose of river flow forecasting.

Frequency distribution charts such as the ones in this study should be an invaluable tool in familiarizing a new forecaster with the thunderstorm regime in Arizona.

As is evident from this study, there is a surprisingly well organized pattern of the diurnal distribution of convective activity. Thunderstorms which begin in the mountains early in the day move gradually toward the deserts. However, there are smaller scale patterns which show through the large picture even when using data from varying flow patterns and different years. The most-pronounced pattern is the maximum frequency area that originates in the White Mountains early in the afternoon and ends up in the deserts east of Phoenix some 8 to 10 hours later. More subtle patterns are also apparent, but there is a definite relationship from year to year in the convective diurnal regime.

The field is wide open for further investigations of this type. Complete 24-hour radar coverage has only been available in Arizona for the summers of 1970 and 1971. Other studies that could be undertaken include the diurnal distribution of convective summertime echoes under different synoptic situations and steering patterns, and comparison of echo distribution under differing stability values and moisture content. Similarly, wintertime storm systems could be studied as to the distribution of precipitation across the state.

## V. REFERENCES


BENNER, H. P., and D. P. SMITH. *Joint ESSA/FAA ARTC Radar Weather Surveillance Program*, U. S. Department of Commerce, Environmental Science Services Administration, Technical Memorandum WBTM WR-35, 1968.

SELLERS, WILLIAM D., and CRISTINE R. GREEN, eds. *Arizona Climate*, University of Arizona Press, Tucson, Arizona, 503 pp (see pp 11-16), 1964.

SMITH, DANIEL L. *The Application of Digitized Radar Data to the Prediction of Summertime Convective Activity in Coastal Regions*, Fourteenth Radar Meteorology Conference, November 17 - 20, 1970, Tucson, Arizona, pp 347-358.

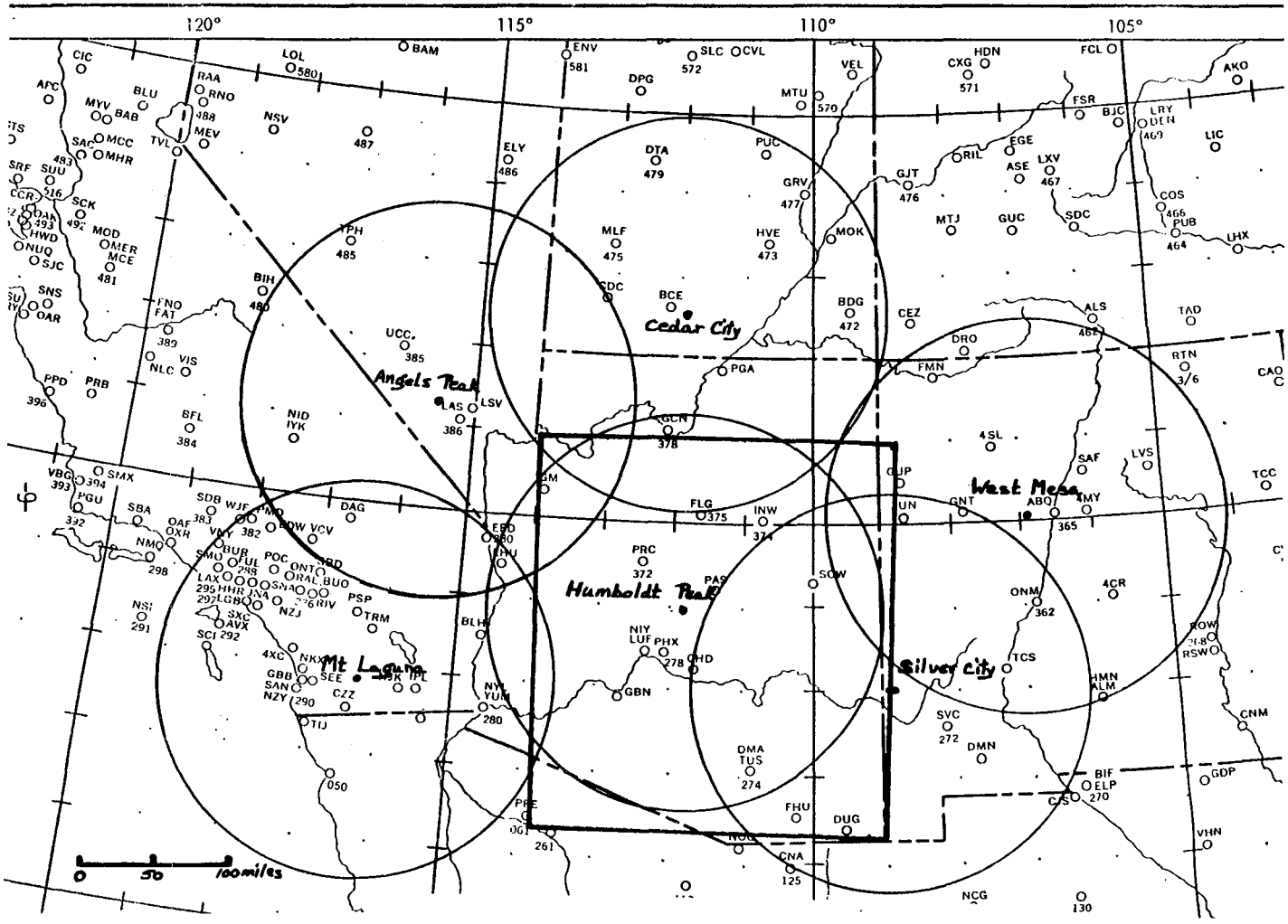


FIGURE 1. LOCATION OF ARTC RADAR SITES USED IN STUDY.

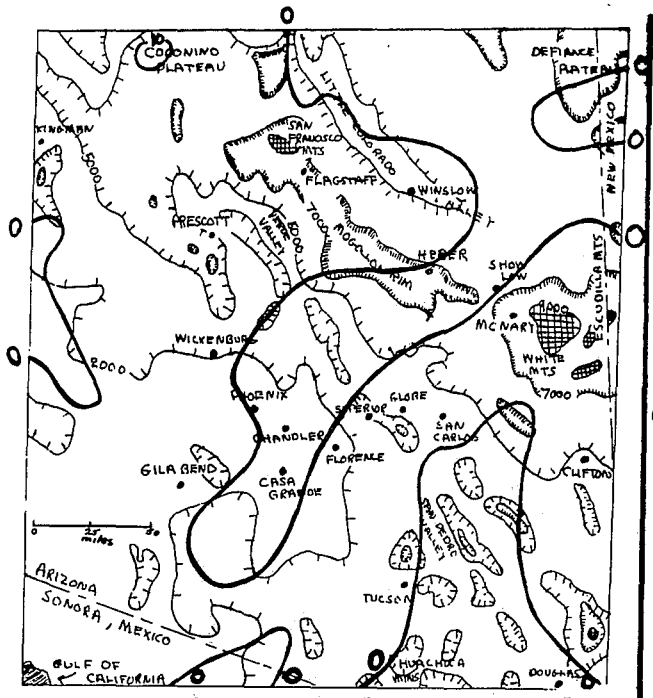


FIGURE 2. FREQUENCY OF RADAR ECHO DETECTION, 0930 MST, JULY-AUGUST 1971.

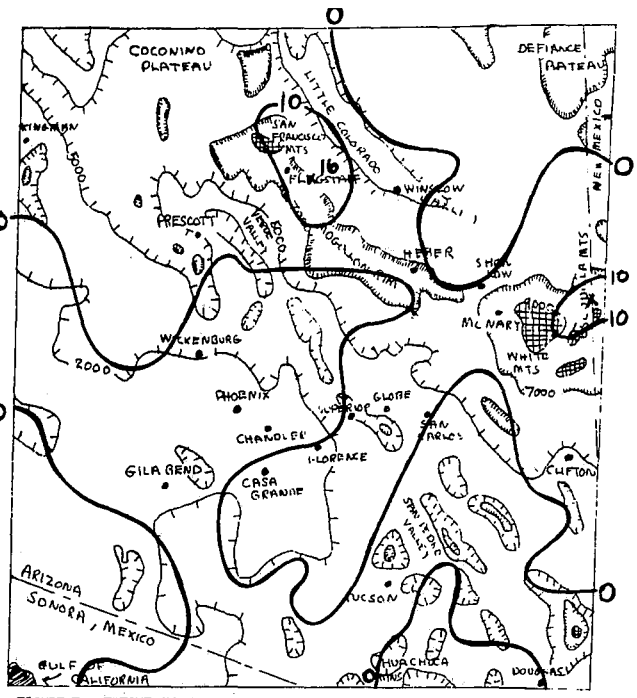


FIGURE 3. FREQUENCY OF RADAR ECHO DETECTION, 1030 MST, JULY-AUGUST 1971.

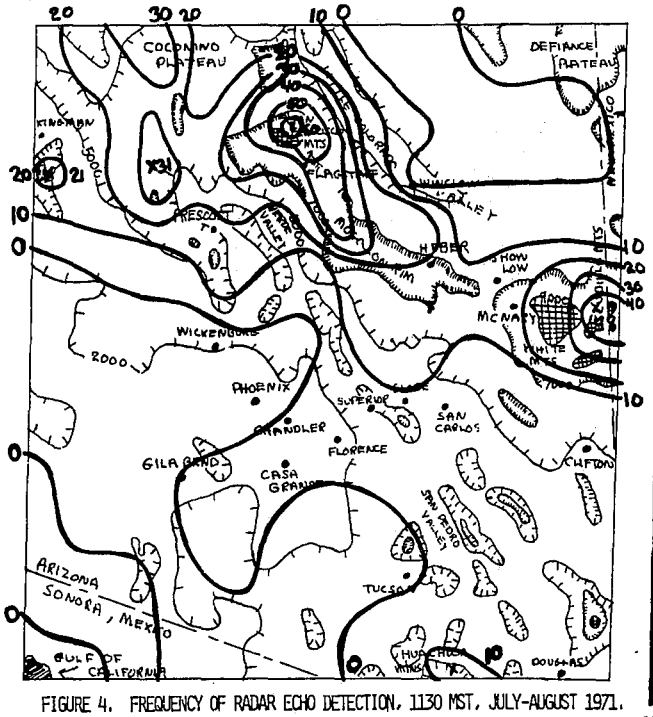


FIGURE 4. FREQUENCY OF RADAR ECHO DETECTION, 1130 MST, JULY-AUGUST 1971.

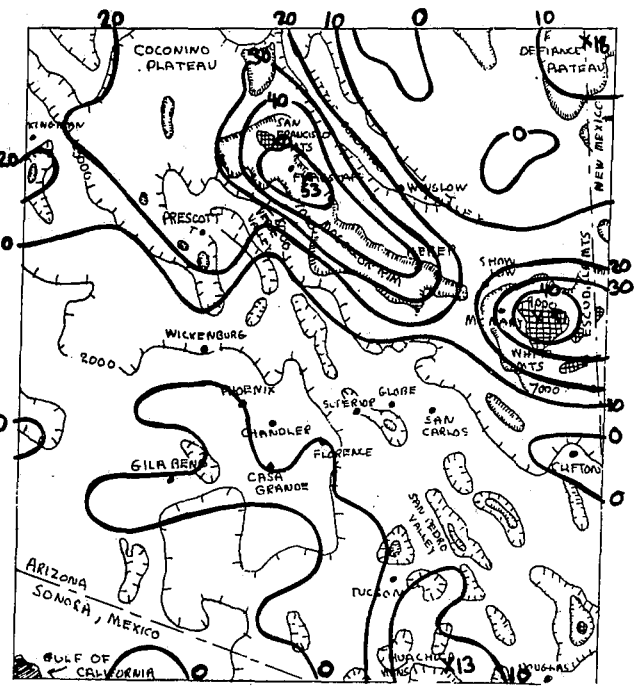


FIGURE 5. FREQUENCY OF RADAR ECHO DETECTION, 1230 MST, JULY-AUGUST 1971.

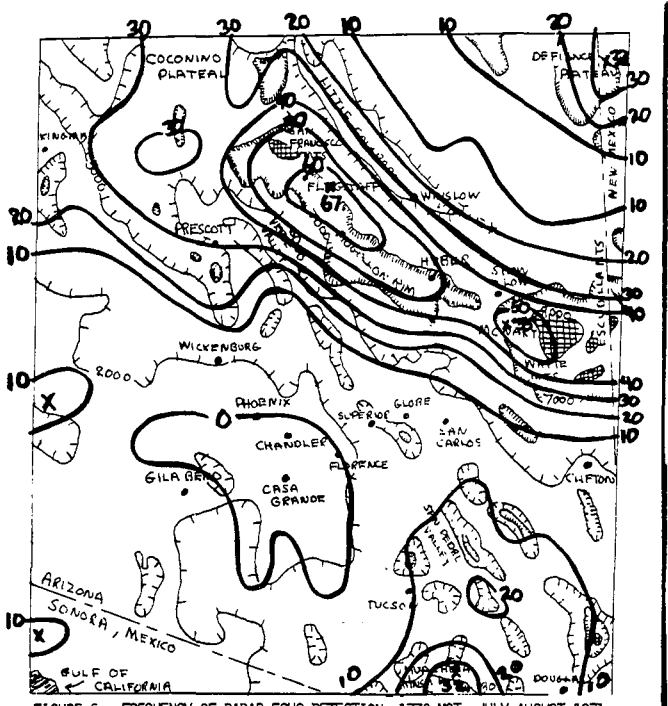


FIGURE 6. FREQUENCY OF RADAR ECHO DETECTION, 1330 MST, JULY-AUGUST 1971.

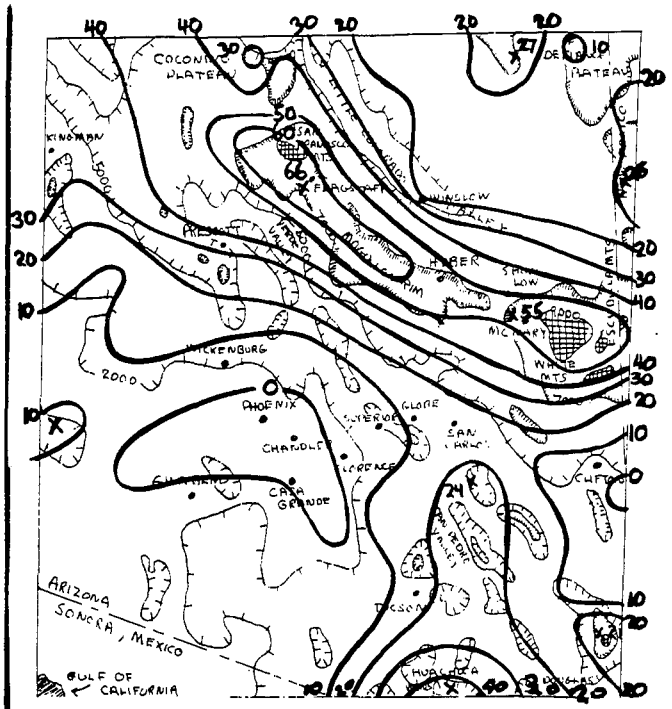


FIGURE 7. FREQUENCY OF RADAR ECHO DETECTION, 1430 MST, JULY-AUGUST 1971.

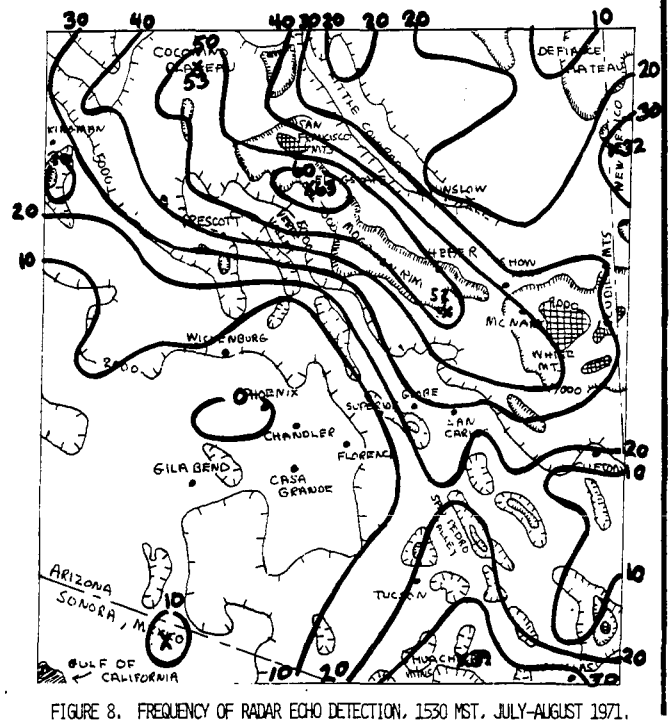


FIGURE 8. FREQUENCY OF RADAR ECHO DETECTION, 1530 MST, JULY-AUGUST 1971.

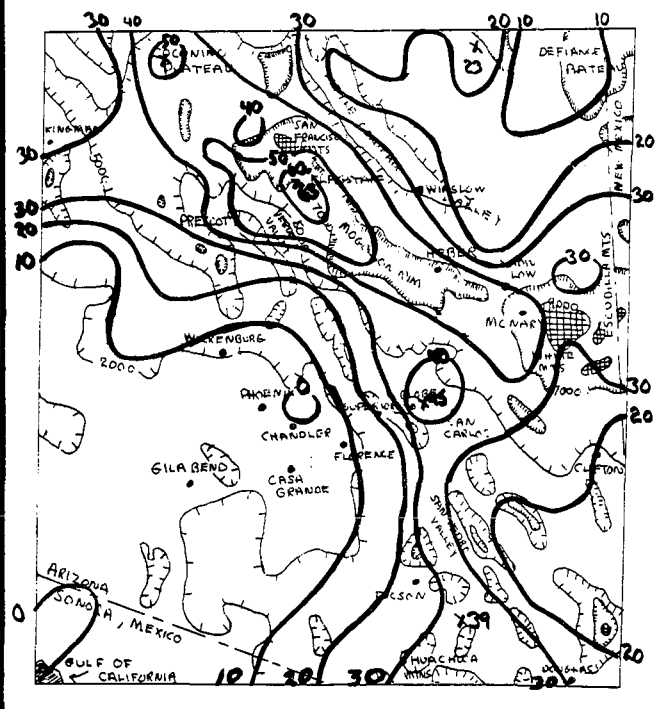


FIGURE 9. FREQUENCY OF RADAR ECHO DETECTION, 1630 MST, JULY-AUGUST 1971.

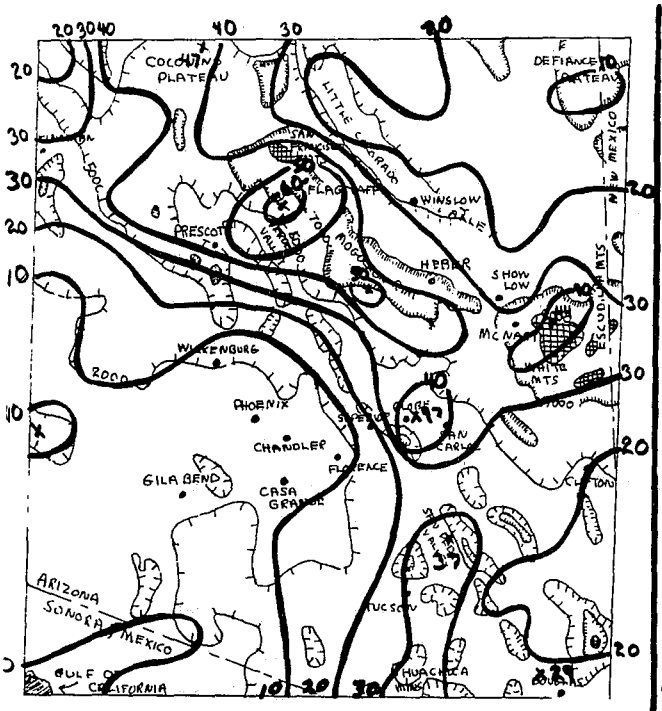


FIGURE 10. FREQUENCY OF RADAR ECHO DETECTION, 1730 MST, JULY-AUGUST 1971.

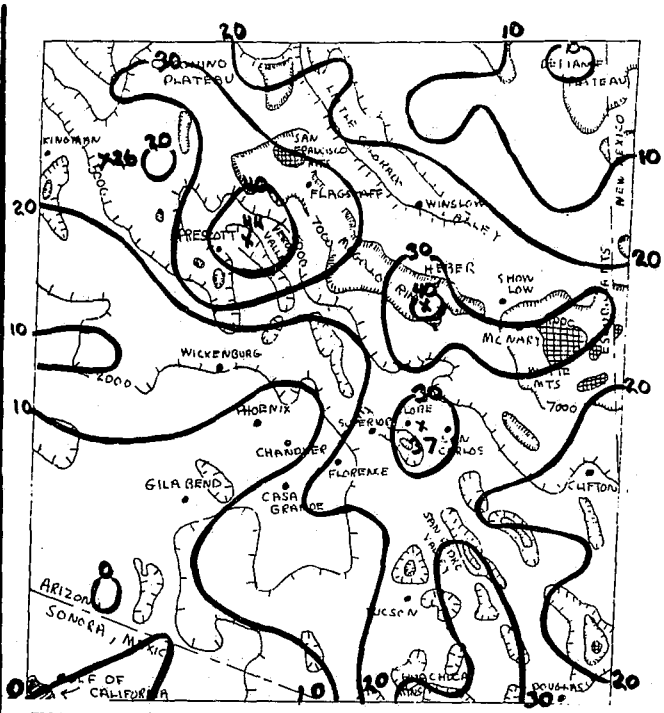


FIGURE 11. FREQUENCY OF RADAR ECHO DETECTION, 1830 MST, JULY-AUGUST 1971.

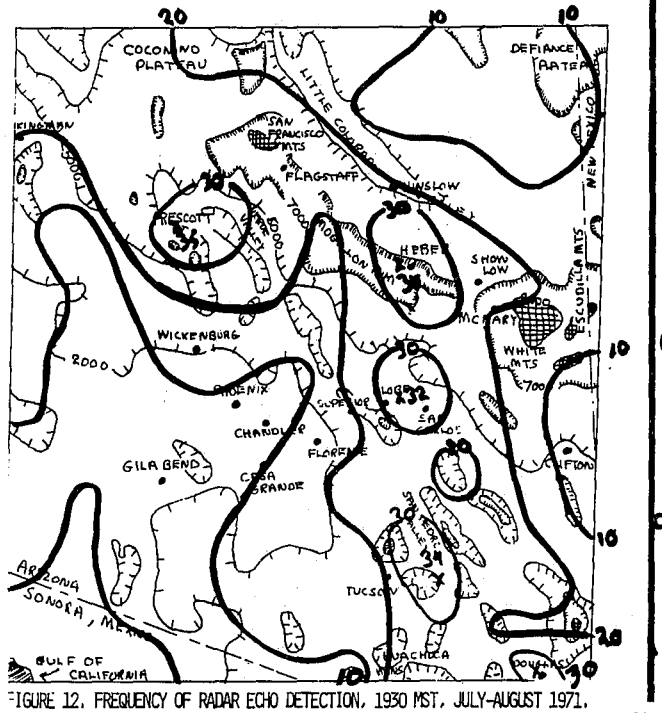


FIGURE 12. FREQUENCY OF RADAR ECHO DETECTION, 1930 MST, JULY-AUGUST 1971.

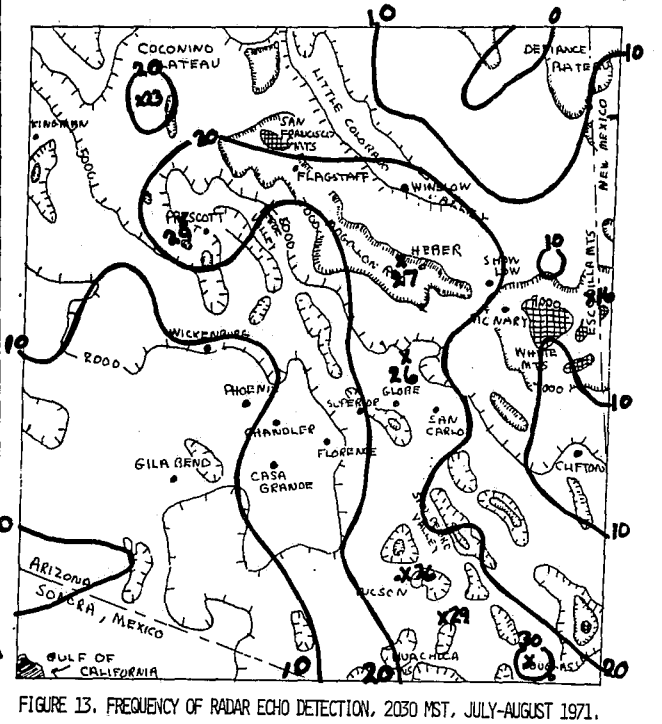


FIGURE 13. FREQUENCY OF RADAR ECHO DETECTION, 2030 MST, JULY-AUGUST 1971.

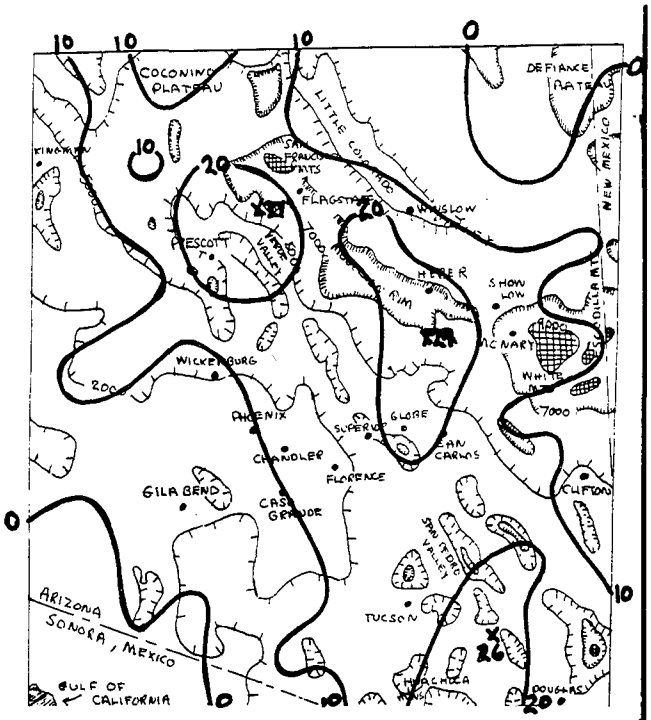


FIGURE 14. FREQUENCY OF RADAR ECHO DETECTION, 2130 MST, JULY-AUGUST 1971.

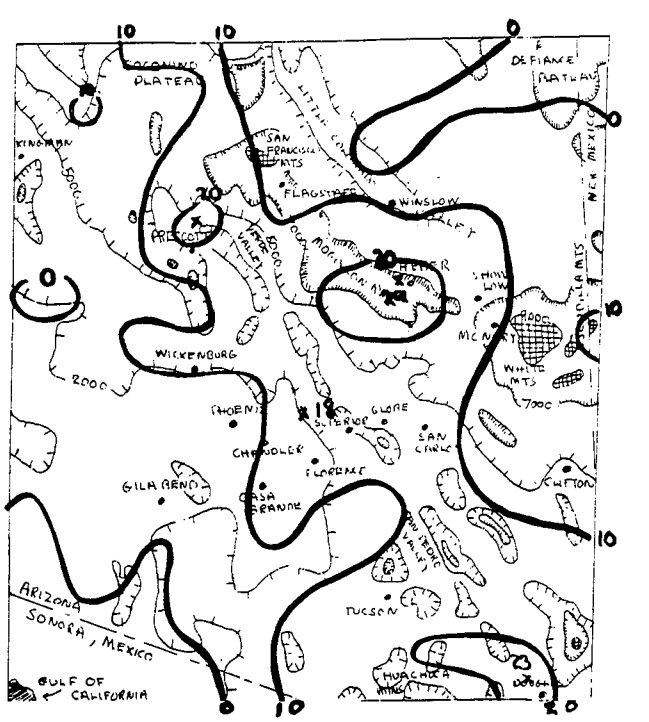


FIGURE 15. FREQUENCY OF RADAR ECHO DETECTION, 2230 MST, JULY-AUGUST 1971.

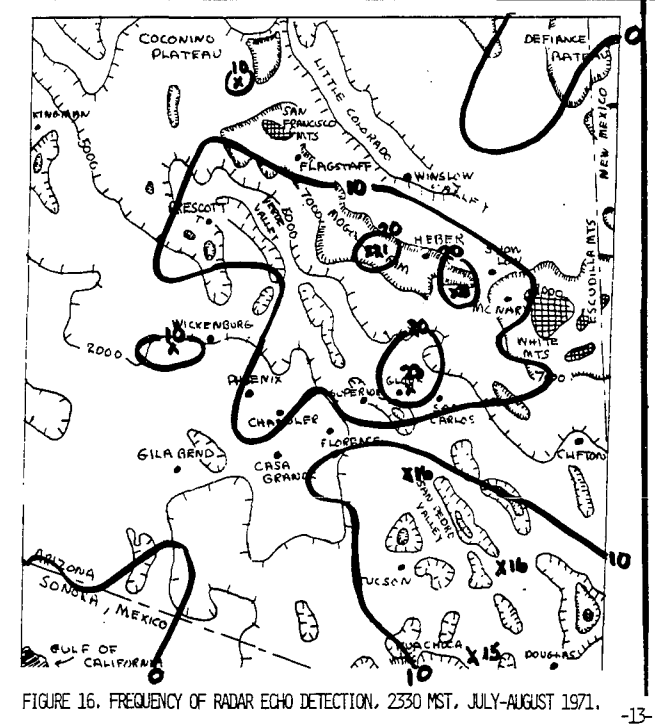


FIGURE 16. FREQUENCY OF RADAR ECHO DETECTION, 2330 MST, JULY-AUGUST 1971.

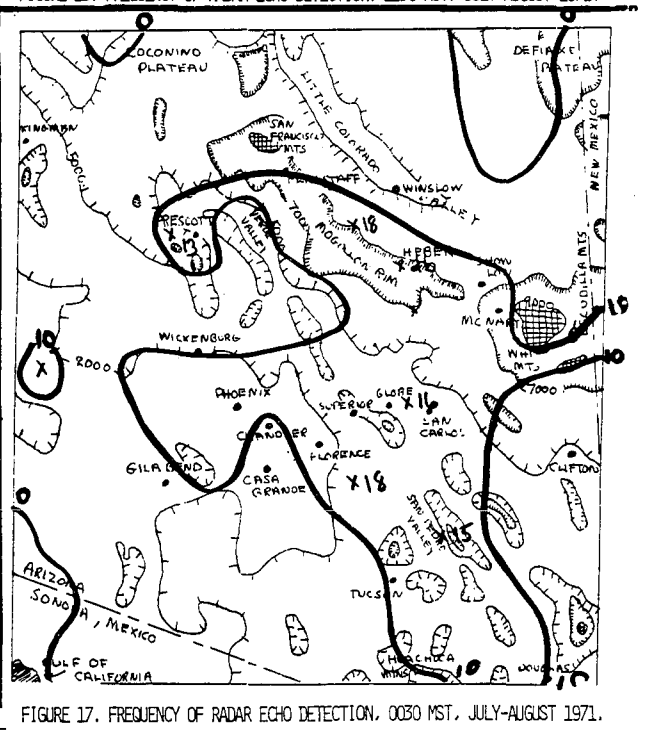


FIGURE 17. FREQUENCY OF RADAR ECHO DETECTION, 0030 MST, JULY-AUGUST 1971.

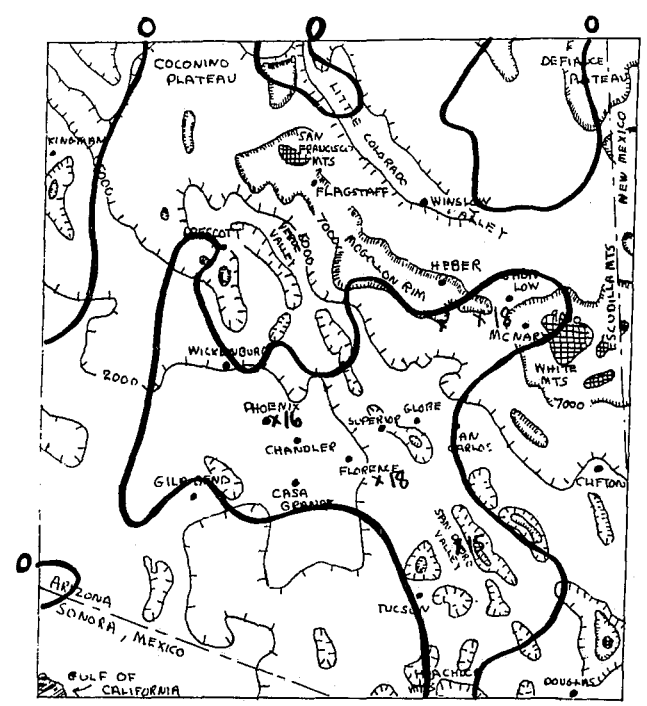


FIGURE 18. FREQUENCY OF RADAR ECHO DETECTION, 0130 MST, JULY-AUGUST 1971.

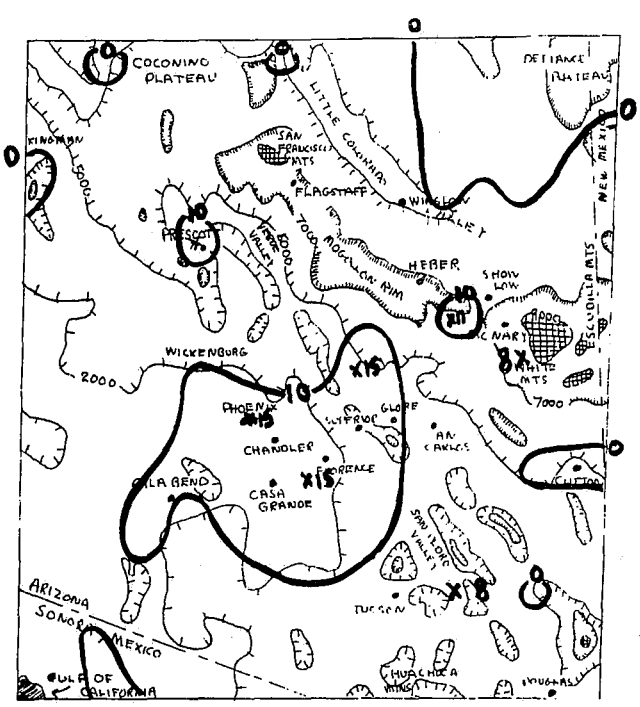


FIGURE 19. FREQUENCY OF RADAR ECHO DETECTION, 0230 MST, JULY-AUGUST 1971.

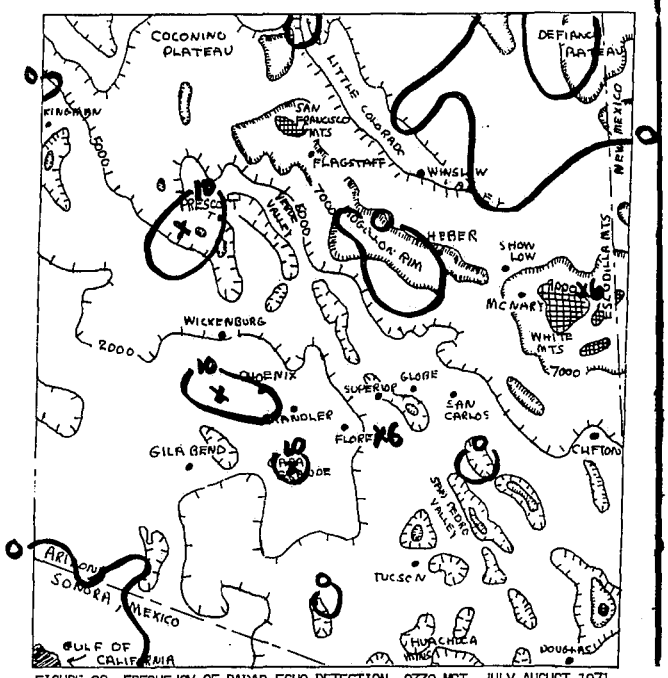


FIGURE 20. FREQUENCY OF RADAR ECHO DETECTION, 0330 MST, JULY-AUGUST 1971.

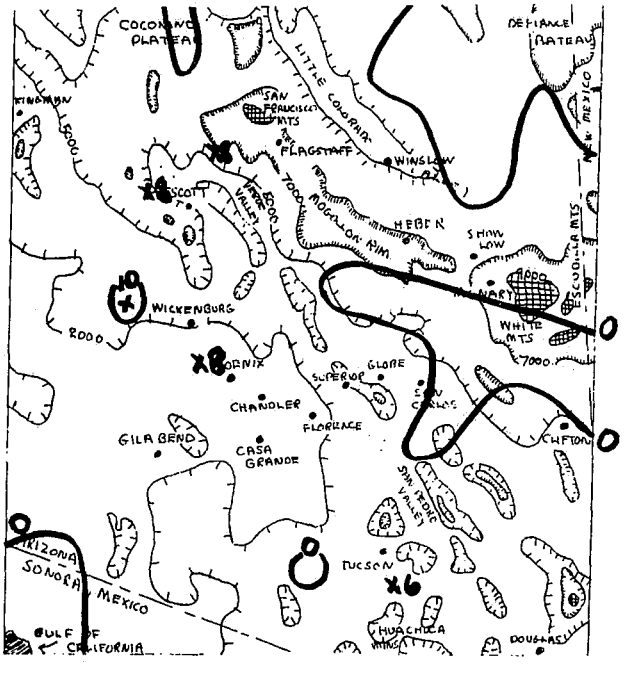


FIGURE 21. FREQUENCY OF RADAR ECHO DETECTION, 0430 MST, JULY-AUGUST 1971.

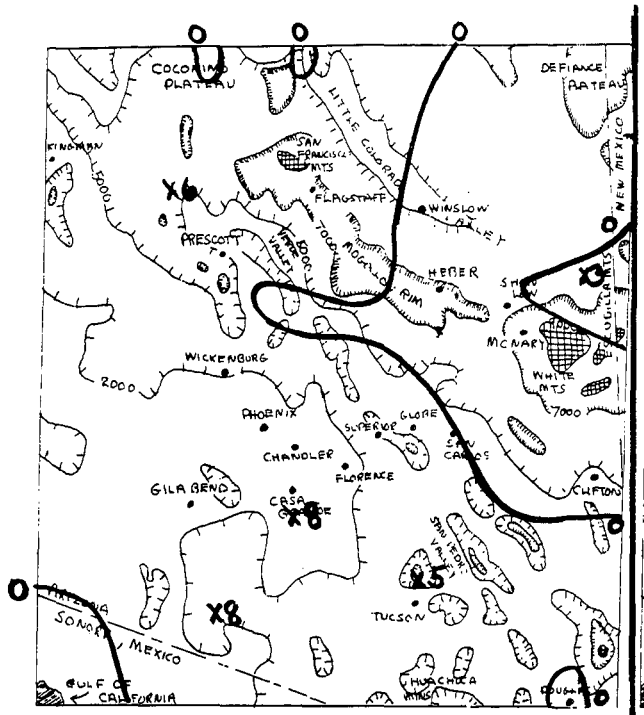

FIGURE 22. FREQUENCY OF RADAR ECHO DETECTION, 0530 MST, JULY-AUGUST 1971.

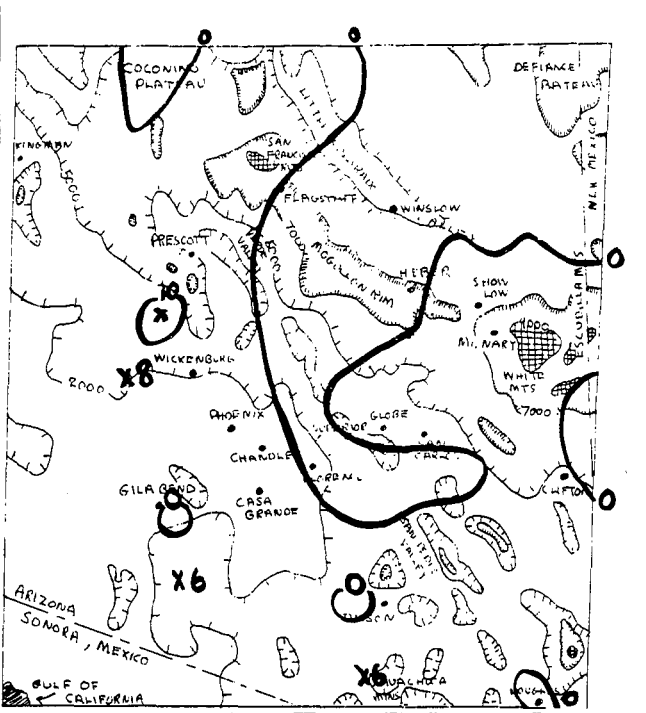

FIGURE 23. FREQUENCY OF RADAR ECHO DETECTION, 0630 MST, JULY-AUGUST 1971.

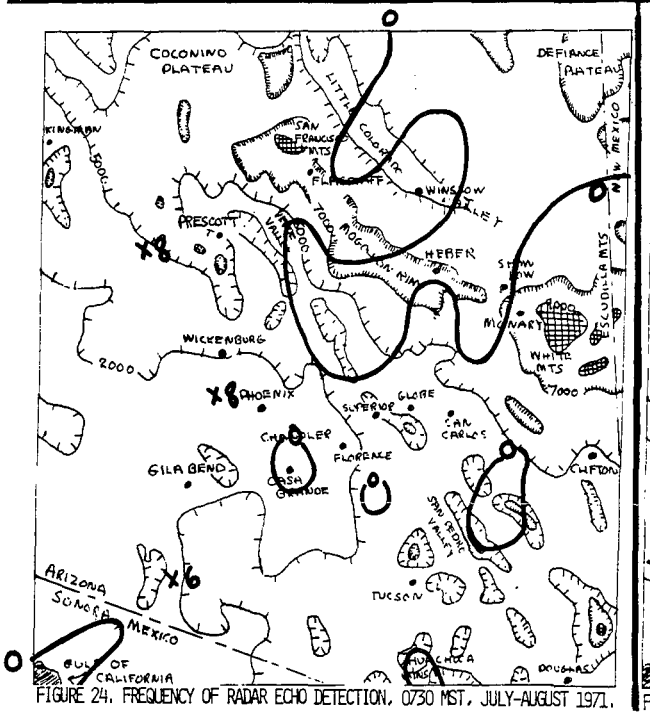

FIGURE 24. FREQUENCY OF RADAR ECHO DETECTION, 0730 MST, JULY-AUGUST 1971.

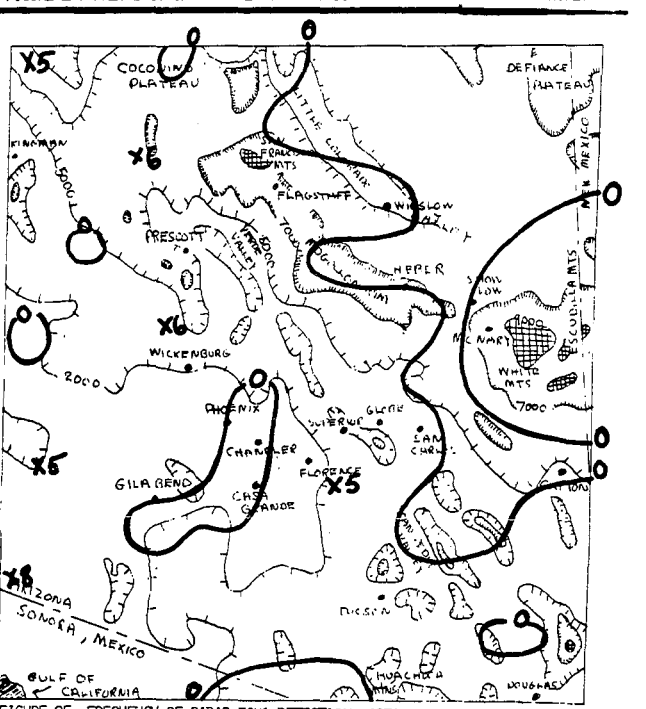

FIGURE 25. FREQUENCY OF RADAR ECHO DETECTION, 0830 MST, JULY-AUGUST 1971.

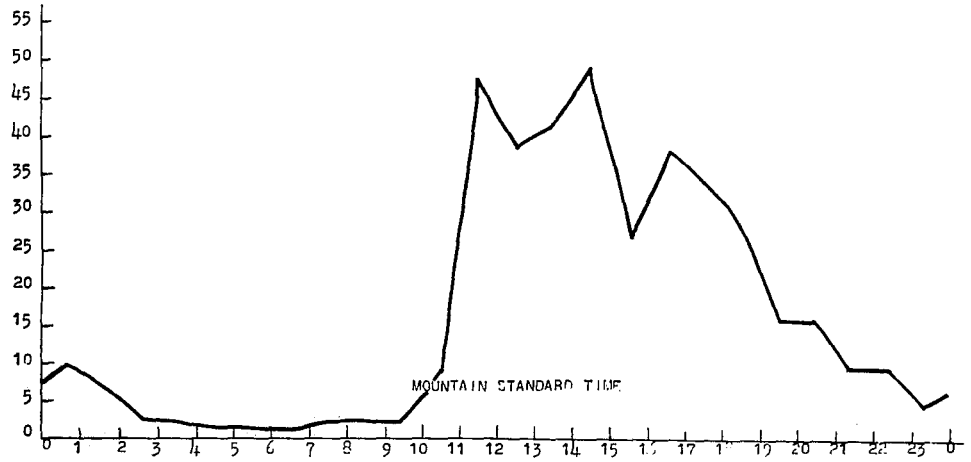


FIGURE 26. HOURLY FREQUENCY OF RADAR ECHOES AT ESCUDILLA MOUNTAIN, JULY-AUGUST 1971.

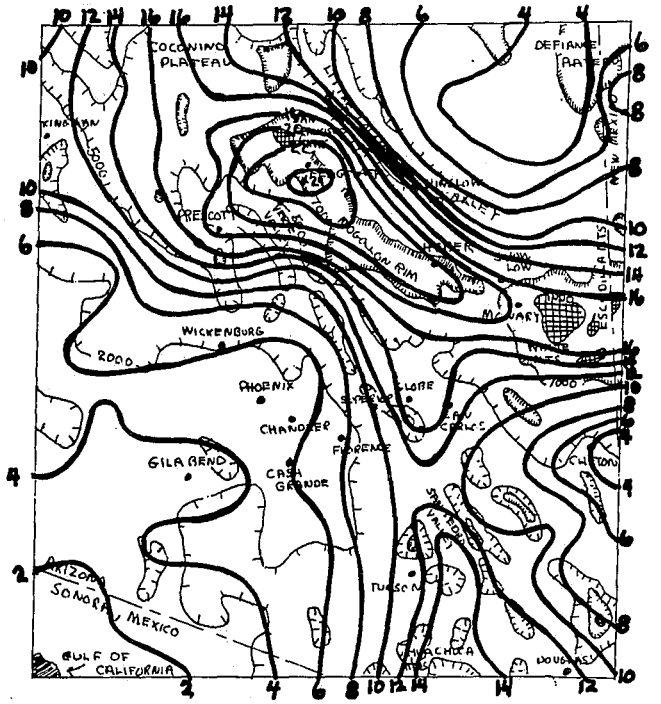


FIGURE 27. TWENTY-FOUR HOUR MEAN ECHO FREQUENCY CHART, JULY-AUGUST 1971.

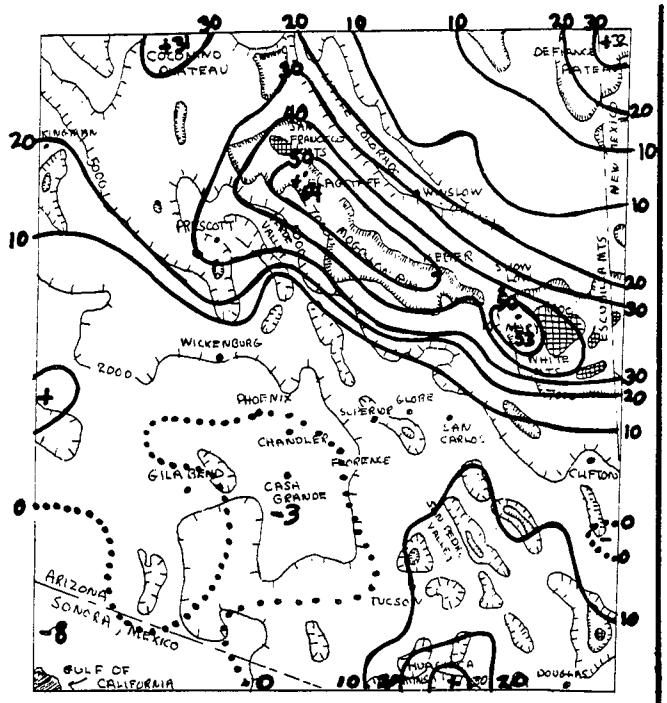


FIGURE 28. THREE-HOUR ECHO FREQUENCY CHANGE CHART, 1330 MST, JULY-AUGUST 1971.

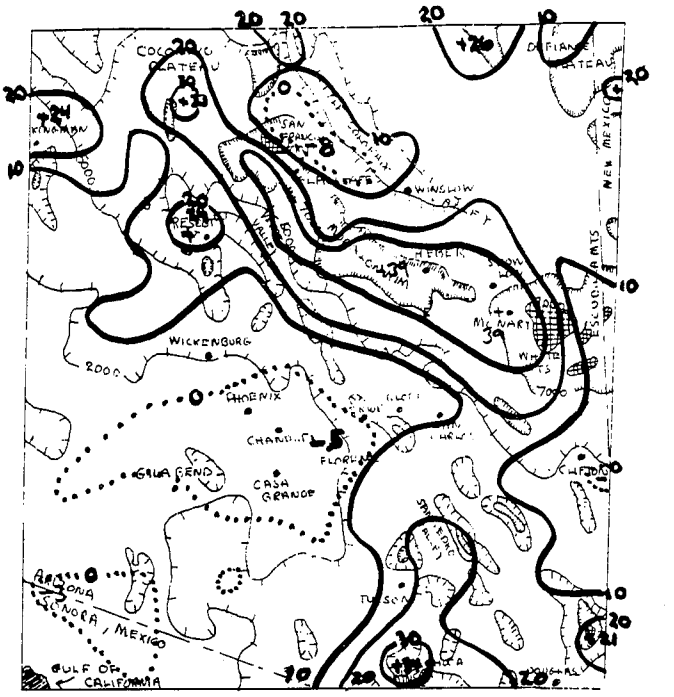


FIGURE 29. THREE-HOUR ECHO FREQUENCY CHANGE CHART, 1430 MST, JULY-AUGUST 1971.

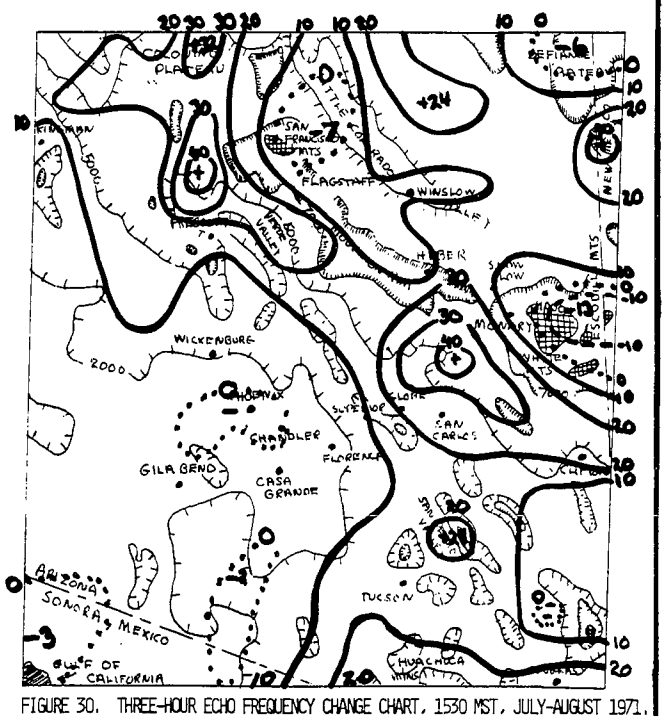


FIGURE 30. THREE-HOUR ECHO FREQUENCY CHANGE CHART, 1530 MST, JULY-AUGUST 1971.

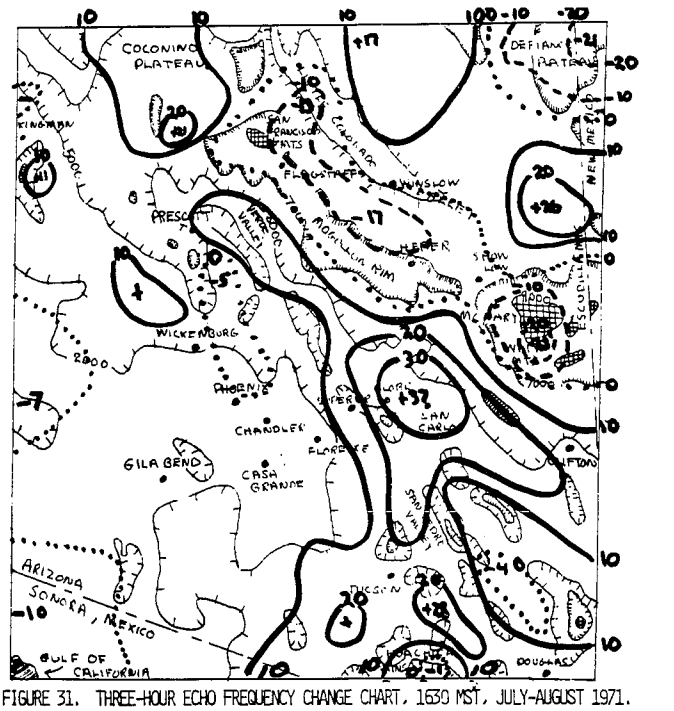


FIGURE 31. THREE-HOUR ECHO FREQUENCY CHANGE CHART, 1630 MST, JULY-AUGUST 1971.

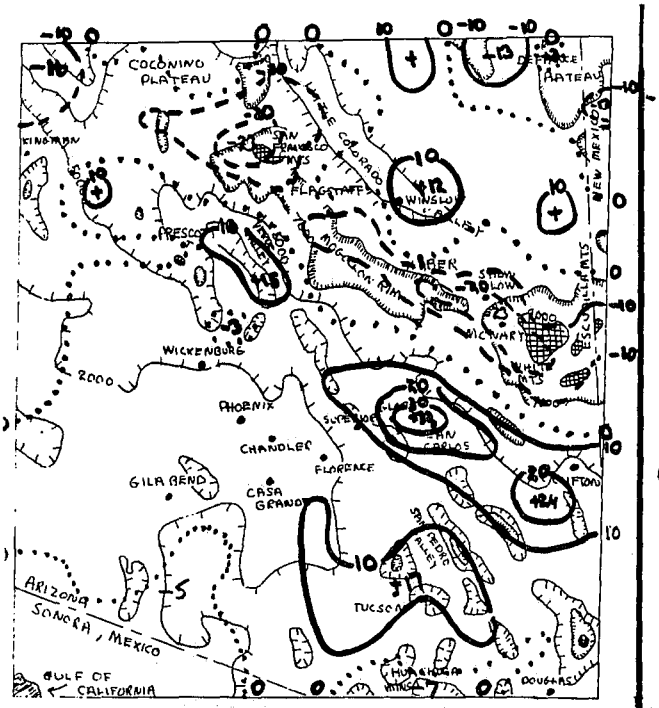


URE 32. THREE-HOUR ECHO FREQUENCY CHANGE CHART, 1730 MST, JULY-AUGUST 1971.

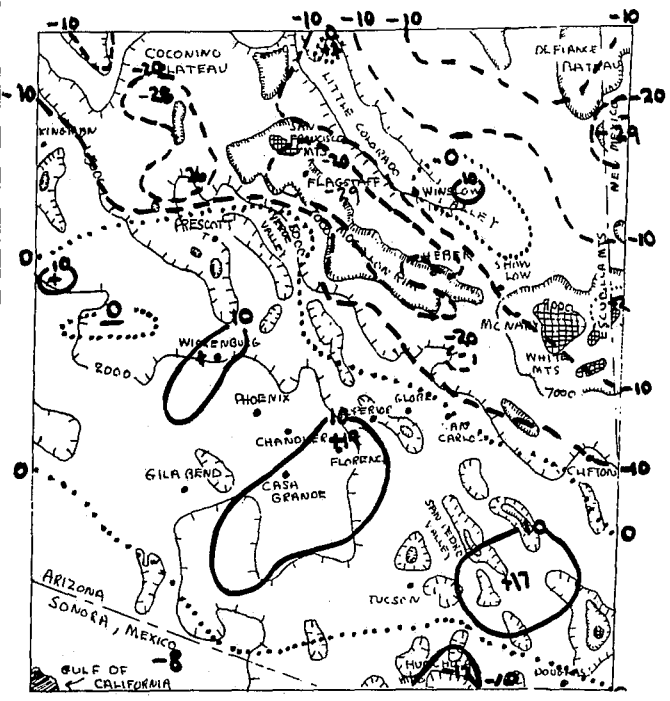


FIGURE 33. THREE-HOUR ECHO FREQUENCY CHANGE CHART, 1830 MST, JULY-AUGUST 1971.

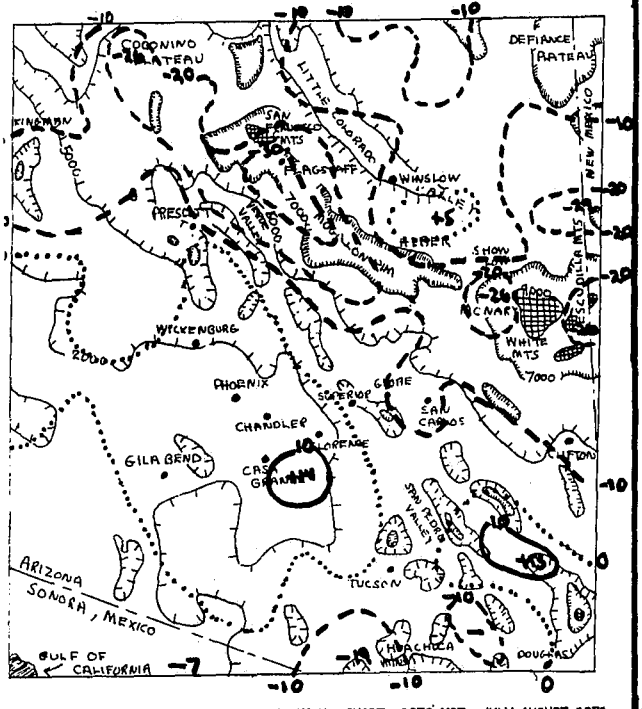


URE 34. THREE-HOUR ECHO FREQUENCY CHANGE CHART, 1930 MST, JULY-AUGUST 1971.

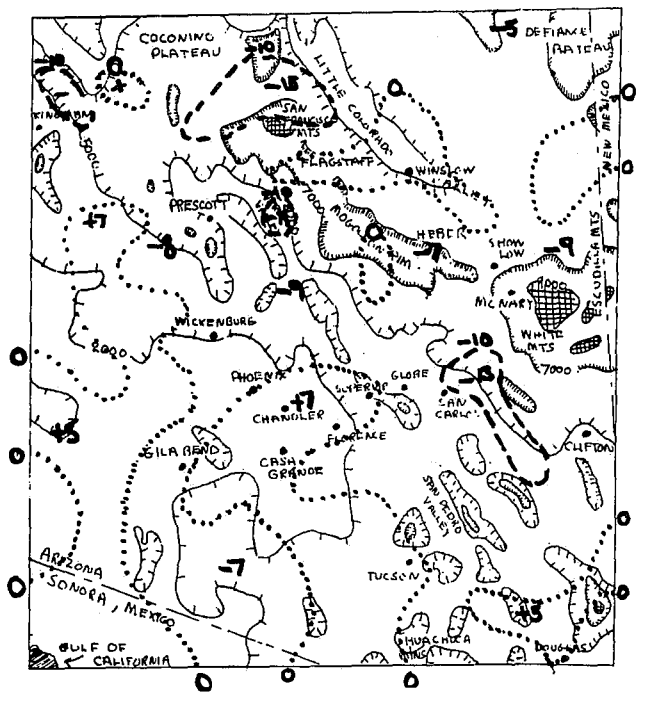


FIGURE 35. THREE-HOUR ECHO FREQUENCY CHANGE CHART, 2030 MST, JULY-AUGUST 1971.

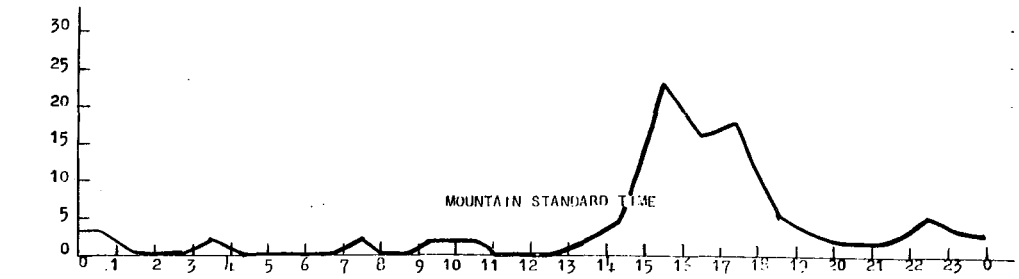


FIGURE 36. HOURLY FREQUENCY RADAR ECHOES, CLIFTON, ARIZONA, JULY-AUGUST 1971.

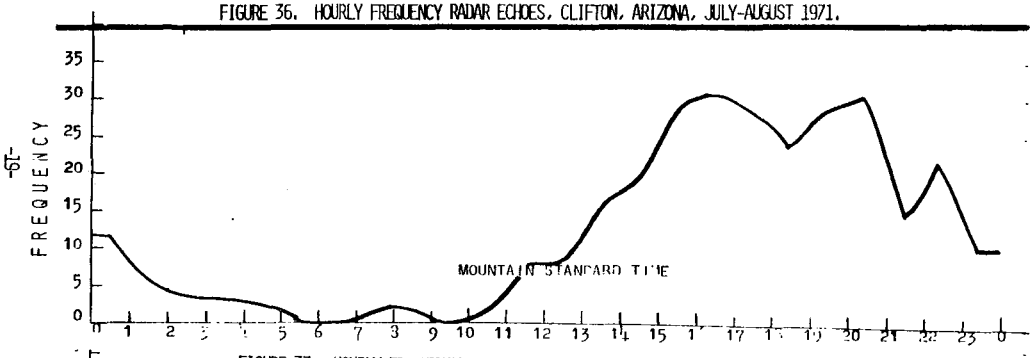


FIGURE 37. HOURLY FREQUENCY RADAR ECHOES, DOUGLAS, ARIZONA, JULY-AUGUST 1971.

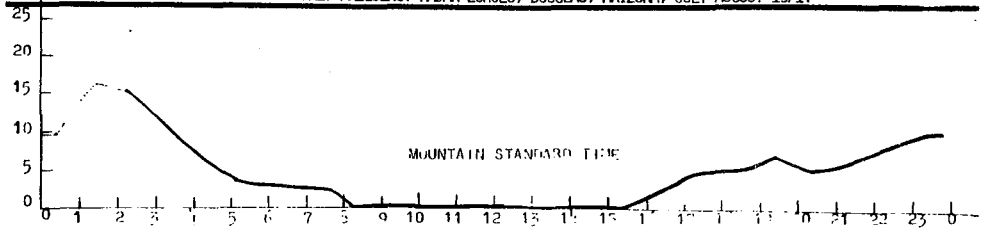


FIGURE 38. HOURLY FREQUENCY RADAR ECHOES, PHOENIX, ARIZONA, JULY-AUGUST 1971.

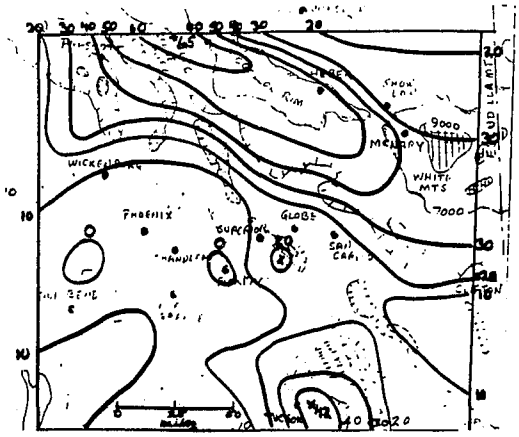


FIGURE 39. FREQUENCY OF RADAR ECHOES, 1430 MST, JULY-AUGUST 1970.

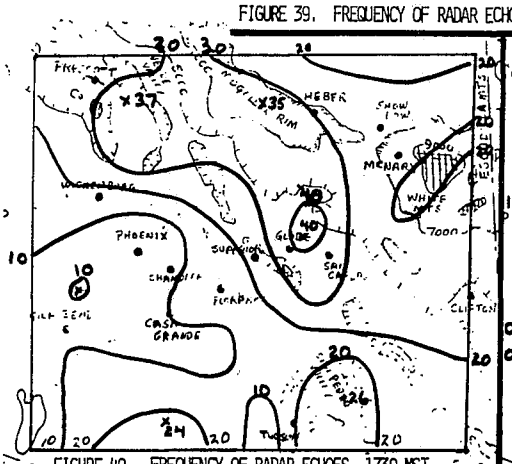


FIGURE 40. FREQUENCY OF RADAR ECHOES, 1730 MST.

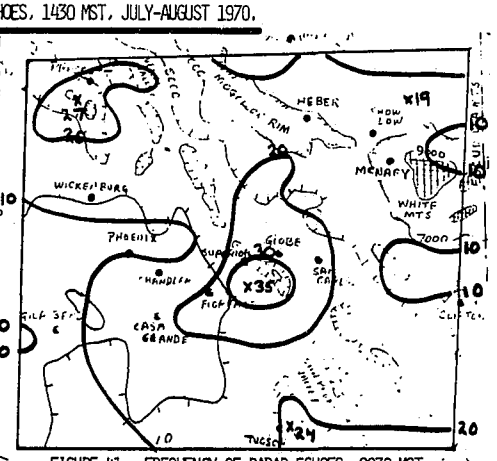


FIGURE 41. FREQUENCY OF RADAR ECHOES, 2030 MST.

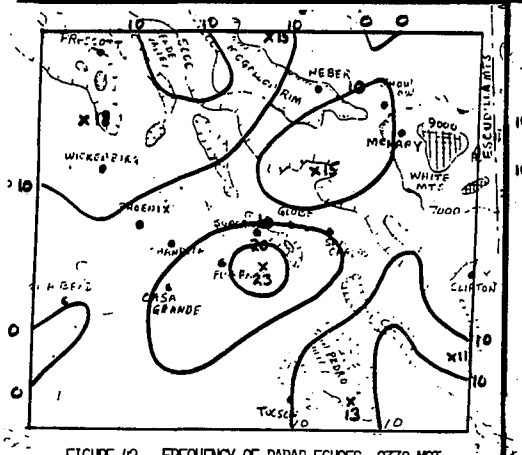


FIGURE 42. FREQUENCY OF RADAR ECHOES, 2330 MST.

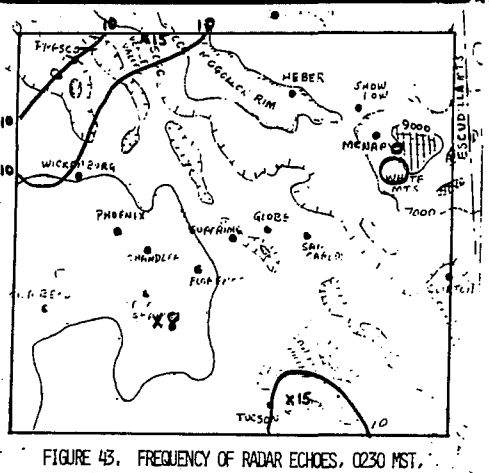


FIGURE 43. FREQUENCY OF RADAR ECHOES, 0230 MST.

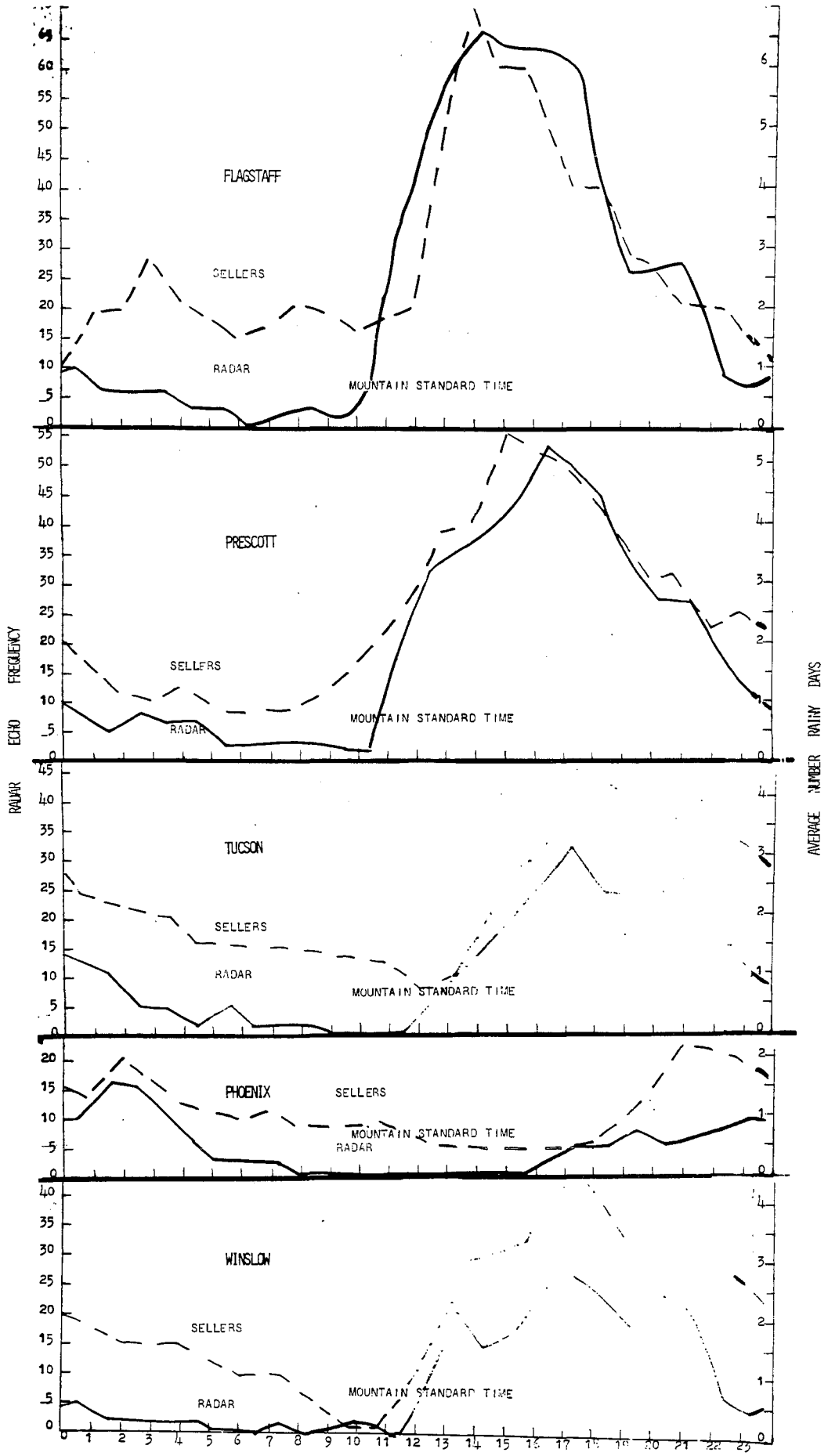


FIGURE 44. HOURLY RADAR ECHO FREQUENCY, JULY-AUGUST 1971 (SOLID LINE) AND AVERAGE NUMBER OF DAYS WITH PRECIPITATION ≥.01 (1948-57) (DASHED LINE), AT FLAGSTAFF, PRESCOTT, TUCSON, PHOENIX, AND WINSLOW (TOP TO BOTTOM).

Western Region Technical Memoranda: (Continued)

No. 45/2 Precipitation Probabilities in the Western Region Associated with Spring 500-mb Map Types. Richard P. Augulis, January 1970. (PB-189434)
No. 45/3 Precipitation Probabilities in the Western Region Associated with Summer 500-mb Map Types. Richard P. Augulis, January 1970. (PB-189414)
No. 45/4 Precipitation Probabilities in the Western Region Associated with Fall 500-mb Map Types. Richard P. Augulis, January 1970. (PB-189435)
No. 46 Applications of the Net Radiometer to Short-Range Fog and Stratus Forecasting at Eugene, Oregon. L. Yee and E. Bates, December 1969. (PB-190476)
No. 47 Statistical Analysis as a Flood Routing Tool. Robert J. C. Burnash, December 1969. (PB-188744)
No. 48 Tsunami. Richard A. Augulis, February 1970. (PB-190157)
No. 49 Predicting Precipitation Type. Robert J. C. Burnash and Floyd E. Hug, March 1970. (PB-190962)
No. 50 Statistical Report on Aeroallergens (Pollens and Molds) Fort Huachuca, Arizona, 1969. Wayne S. Johnson, April 1970. (PB-191743)
No. 51 Western Region Sea State and Surf Forecaster's Manual. Gordon C. Shields and Gerald B. Burdwell, July 1970. (PB-193102)
No. 52 Sacramento Weather Radar Climatology. R. G. Pappas and C. M. Veliquette, July 1970. (PB-193347)
No. 53 Experimental Air Quality Forecasts in the Sacramento Valley. Norman S. Benes, August 1970. (PB-194128)
No. 54 A Refinement of the Vorticity Field to Delineate Areas of Significant Precipitation. Barry B. Aronovitch, August 1970.
No. 55 Application of the SSARR Model to a Basin Without Discharge Record. Vail Schermerhorn and Donald W. Kuehl, August 1970. (PB-194394)
No. 56 Areal Coverage of Precipitation in Northwestern Utah. Philip Williams, Jr., and Werner J. Heck, September 1970. (PB-194389)
No. 57 Preliminary Report on Agricultural Field Burning vs. Atmosphere Visibility in the Willamette Valley of Oregon. Earl M. Bates and David O. Chilcote, September 1970. (PB-194710)
No. 58 Air Pollution by Jet Aircraft at Seattle-Tacoma Airport. Wallace R. Donaldson, October 1970. (COM-71-00017)
No. 59 Application of P.E. Model Forecast Parameters to Local-Area Forecasting. Leonard W. Snellman, October 1970. (COM-71-00016)

NOAA Technical Memoranda NWS

No. 60 An Aid for Forecasting the Minimum Temperature at Medford, Oregon. Arthur W. Fritz, October 1970. (COM-71-00120)
No. 61 Relationship of Wind Velocity and Stability to $SO_2$ Concentrations at Salt Lake City, Utah. Werner J. Heck, January 1971. (COM-71-00232)
No. 62 Forecasting the Catalina Eddy. Arthur L. Eichelberger, February 1971. (COM-71-00223)
No. 63 700-mb Warm Air Advection as a Forecasting Tool for Montana and Northern Idaho. Norris E. Woerner, February 1971. (COM-71-00349)
No. 64 Wind and Weather Regimes at Great Falls, Montana. Warren B. Price, March 1971.
No. 65 Climate of Sacramento, California. Wilbur E. Figgins, June 1971. (COM-71-00764)
No. 66 A Preliminary Report on Correlation of ARTCC Radar Echoes and Precipitation. Wilbur K. Hall, June 1971. (COM-71-00829)
No. 67 Precipitation Detection Probabilities by Los Angeles ARTC Radars. Dennis E. Ronne, July 1971. (COM-71-00925)
No. 68 A Survey of Marine Weather Requirements. Herbert P. Benner, July 1971. (COM-71-00889)
No. 69 National Weather Service Support to Soaring Activities. Ellis Burton, August 1971. (COM-71-00956)
No. 70 Predicting Inversion Depths and Temperature Influences in the Helena Valley. David E. Olsen, October 1971. (COM-71-01037)
No. 71 Western Region Synoptic Analysis-Problems and Methods. Philip Williams, Jr., February 1972. (COM-72-10433)
No. 72 A Paradox Principle in the Prediction of Precipitation Type. Thomas J. Weitz, February 1972. (COM-72-10432)
No. 73 A Synoptic Climatology for Snowstorms in Northwestern Nevada. Bert L. Nelson, Paul M. Fransioli, and Clarence M. Sakamoto, February 1972. (COM-72-10338)
No. 74 Thunderstorms and Hail Days Probabilities in Nevada. Clarence M. Sakamoto, April 1972. (COM-72-10554)
No. 75 A Study of the Low Level Jet Stream of the San Joaquin Valley. Ronald A. Willis and Philip Williams, Jr., May 1972.
No. 76 Monthly Climatological Charts of the Behavior of Fog and Low Stratus at Los Angeles International Airport. Donald M. Gales, July 1972.